

Supporting Information

Cheap Carbon Black-based High-performance Electrocatalysts for Oxygen Reduction Reaction

Ping Song, Yuwei Zhang, Jing Pan, Lin Zhuang and Weilin Xu*

E-mail: weilinxu@ciac.ac.cn

1. Experimental

1.1. Materials

The carbon black BP2000 was purchased from Asian-Pacific Specialty Chemicals Kuala Lumpur, Urea ($\text{CH}_4\text{N}_2\text{O}$) and ferric chloride hexahydrate ($\text{FeCl}_3 \cdot 6\text{H}_2\text{O}$) were purchased from Sinopharm Chemical Reagent Co. LTD, Potassium hydroxide (KOH) was purchased from Beijing Chemical Works, and Nafion solution (5 wt %) were obtained from Sigma-Aldrich. All the chemicals were used as delivered without further treatment. Ultrapure water with the specific resistance of $18.23 \text{ M}\Omega \cdot \text{cm}$ was obtained by reversed osmosis followed by ion-exchange and filtration. Rotating disk electrode of glassy carbon (RDE, 4 mm in diameter) was purchased from Tianjin Aida Hengsheng Tech. Co., China.

1.2. Preparation of nitrogen, Fe-co-doped carbon materials

The synthesis of BP_{ox} was obtained by a certain BP2000 with 6M HNO_3 stirred when refluxing at 80°C for 6 hours. Then Centrifugal washing was done with ultrapure water many times until the solution is neutral. Final the solid is grinded when it was dried at 60°C in drying oven.

The synthesis of $\text{BP}_{\text{ox}}\text{-NFe}$ was based on a two-step procedure with BP_{ox} , urea ($\text{CH}_4\text{N}_2\text{O}$) and ferric chloride hexahydrate as initial materials. Firstly, BP_{ox} -based mixtures were obtained as follows: a given amount of BP_{ox} and ferric chloride hexahydrate were mixed in water and then dried to get a $\text{BP}_{\text{ox}}\text{-Fe}$ mixture, and then add in different amount of urea and ground together in an agate mortar for about half an hour. After that the pyrolysis of the obtained mixture was performed at 900°C for 1 h under argon atmosphere with flow rate of $80 \text{ mL}/\text{min}$. For comparison, $\text{BP}_{\text{ox}}\text{-N}$ was also obtained in a similar way without ferric chloride hexahydrate. These catalysts can be reproduced easily.

1.3. Characterization of the nitrogen, Fe-doped carbon materials

X-ray photoelectron spectroscopic (XPS) measurements were performed on a AXIS Ultra DLD (Kratos company) using a monochromic Al X-ray source. The

morphology and dimensions of as-prepared samples were obtained using transmission electron microscopy (TEM) obtained on a JEM-2100F microscopy with an accelerating voltage of 200 kV. The Brunauer-Emmett-Teller (BET) surface areas and pore volumes were obtained from 77 K N₂ sorption isotherms using ASAP 2020 instrument. The final Fe contents in the catalysts were obtained from ICP-MS (ICAP-6000, Thermo Fisher Scientific). The final N content was determined by element analysis by varioEL cube (elementar analysensysteme GmbH).

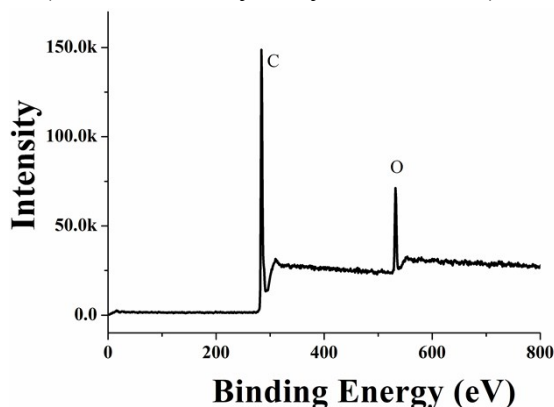


Figure S1. Survey scan of XPS spectrum for BP_{ox}.

1.4. Electrochemical measurements

The activity for the oxygen reduction reaction (ORR) was evaluated by voltamperometry on the high-surface-area NFe-doped carbon material electrodes. Fabrication of the working electrodes was done by pasting catalyst inks on a glassy carbon rotating disk electrode (4 mm in diameter). Its apparent surface area (0.1256 cm²) was used to normalize the ORR activity of the catalysts. The carbon ink was formed by mixing 5 mg of doped carbon materials catalysts, 50 μL of a 5 wt % Nafion solution in alcohol, and 950 μL of ethanol in a plastic vial under ultrasonication. A 10-μL aliquot of the carbon ink was dropped on the surface of the glassy carbon rotating disk electrode, yielding an approximate catalyst loading of 0.39 mg·cm⁻². For comparison, a commercially available platinum/carbon catalyst, nominally 20 wt % on carbon black from E-TEK was used. The platinum based ink was obtained by mixing 1 mg catalyst, 50 μL of a 5 wt % Nafion solution in alcohol, 950 μL of ethanol. Then, a 15-μL aliquot of the platinum ink was dropped on the glassy carbon rotating disk electrode, yielding an approximate loading of 0.015 mg or 24 μg Pt cm⁻². The electrolyte was 0.1 M KOH solution; the counter and the reference electrodes were a carbon and a SCE electrode, respectively. The potential of the electrode was controlled by an EG&G (model 273) potentiostat/galvanostat system. Cyclic voltammetry was performed from 0.2 to -1.2 V at 50 mV s⁻¹ after purging the electrolyte with O₂ or N₂ gas for 30 min. Voltamperometry measurements were performed by using the rotating ring disk electrode (RRDE) at different rotating speeds from 225 to 1600 rpm in an O₂-saturated electrolyte from 0.2 to -1.2 V (vs SCE) at a sweep rate of 5 mV/s. In this work the onset potential was defined as the

potential at which the ORR current is 5% of the diffusion-limited current (*Electrochem. Commun.* **2010**, *12*, 628–631).

Koutecky-Levich equation was used for analyzing the transferred electron number (n) during the ORR with disk currents.

$$\frac{1}{j} = \frac{1}{j_L} + \frac{1}{j_K} = \frac{1}{B\omega^{1/2}} + \frac{1}{j_K}$$

$$B = 0.2nFC_{O_2}D_{O_2}^{2/3}\nu^{-1/6}$$

Where j is the overall current density, j_L is the diffusion-limiting current density, J_k is the kinetic current density, ω is the rotation speed, F is the Faraday constant (96485 C mol⁻¹), C_{O_2} is the bulk concentration of O₂ (1.2 x10⁻⁶ mol cm⁻³), D_{O_2} is the diffusion coefficient of O₂ (1.9 x 10⁻⁵ cm² s⁻¹), ν is the kinematics viscosity of the electrolyte (0.01 cm² s⁻¹) and n is the transferred electron numbers in the ORR. The constant 0.2 is adopted when the rotation speed is expressed in rpm.

For the calculation of yields of H₂O₂ on different catalysts, based on both ring and disk currents from RRDE, the percentage of HO₂⁻ generated from ORR and the electron transfer number (n) were estimated by the following equations:

$$(1) HO_2^- \% = 200 \times \frac{i_R/N}{i_D + i_R/N}$$

$$(2) n = 4 \times \frac{i_D}{i_D + i_R/N}$$

Where i_D is the disk current density, i_R is the ring current density and N is the current collection efficiency of the Pt ring disk. N was 0.37 from the reduction of K₃Fe [CN]₆. All the current densities have already been normalized to the electrode surface area.

1.5. Membrane assembly electrode (MEA) preparation and fuel cell tests

In this work, a self-aggregated alkaline polymer electrolyte (aQAPS) was used to prepare anion-exchange membrane with thickness of about 40 μ m for alkaline direct methanol fuel cells tested here. (*Chem. Commun.* **2010**, *46*, 8597-8599). Before fabrication of MEA, the membrane was soaked in 2 M KOH for at least one week to change it to OH⁻. The membrane was then rinsed and stored in Millipore water two days before later use. Its hydroxide ion conductivity is above 10⁻²S/cm at room temperature. Carbon supported Pt (20 or 60 wt % on Vulcan XC72, E-TEK, USA) or BP-NFe was used to prepare the catalyst ink. Inks were made by mixing the catalysts powder, ethanol and 5% Nafion (Aldrich, USA) suspension. The catalyst layer was prepared on non-wet-proofed Toray 90 carbon paper (E-TEK, USA). After the desired amount of catalyst loading was achieved, the anode, cathode and membrane were sandwiched together and pressed at 130 kg/cm² for 5 min at room temperature.

A stainless steel cell consisting of two compartments with 2 mm parallel channel flow field for methanol and oxygen flow was employed in this work. The active cross-section area of the cell was 6.25 cm². The fuel used was 2 M methanol in 2 M KOH at an operation temperature of 60°C, unless otherwise specified. A peristaltic pump (Watson Marlow, UK) was used to supply methanol to anode. The pure dry oxygen was supplied to the cathode with a flow rate of 100 mL/min. An in-house-made water bath and temperature controller were used to maintain the temperature at 60°C. The open circuit voltages (OCV) were recorded after stable values were reached. In order to remove the anode polarization, we had used high-loading Pt/C (60 wt %, 3 mg_{Pt}/cm²) based anode. All the cell polarization data and stability data were obtained after 24h of cell conditioning.

As for the alkaline H₂-O₂ fuel cell reported in this work, a self-aggregated alkaline polymer electrolyte (*a*QAPS) was used to prepare anion-exchange membrane (with thickness of about 50 μm) and ionomer solution for alkaline H₂-O₂ fuel cells tested here. Carbon supported Pt (60 wt % on Vulcan XC72, Jonhson Matthey) or OxBP-Fe was used to prepare the catalyst ink. Inks were made by mixing the catalysts powder, propanol and *a*QAPS solution. The weight percentage of *a*QAPS-S₈ in both the anode and the cathode was calculated to be 20wt%. The catalyst inks were sprayed on each side of the *a*QAPS membrane (Cl⁻ as anion) to the catalyst-coated membrane (CCM). By immersing the CCM in 1 mol/L KOH solution for 24 hours at room temperature, the OH⁻-form CCM was achieved. The CCM was pressed between two pieces of carbon paper (AvCarb GDS3250) to make the membrane electrode assembly (MEA). A H₂-O₂ fuel cell was tested (850e Multi Range, Scribner Associates Co.) under a galvanic mode using fully humidified H₂ and O₂ gases flowing at a rate of 250 mL/min and at temperature of 50°C. The related humidity for both H₂ and O₂ was 100%, and the backpressure was 0 Mpa.

1.6. The effect of oxidation on electrocatalytic performance of pure BP in 0.1 M KOH.

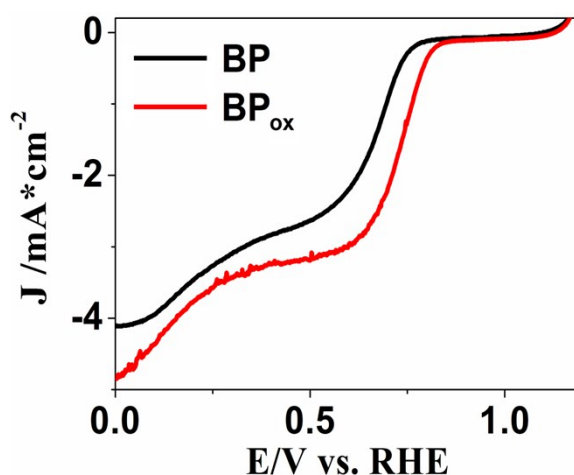


Figure S2. LSVs for oxygen reduction on pristine and oxidized BP in O₂-saturated 0.1 M KOH with rotation speed of 1600 rpm with scan rate of 5 mV/s.

From above it can be seen, the oxidation pretreatment can improve the ORR activity of carbon indicated by the 80mV positive shift of E_{onset} although it is still a two-step two-electron ORR process. The reason for the improvement probably could be attributed to the oxygen species induced on carbon surface and the removal of some unstable amorphous carbon.

2. The dependence of final N content on initial C/U ratio.

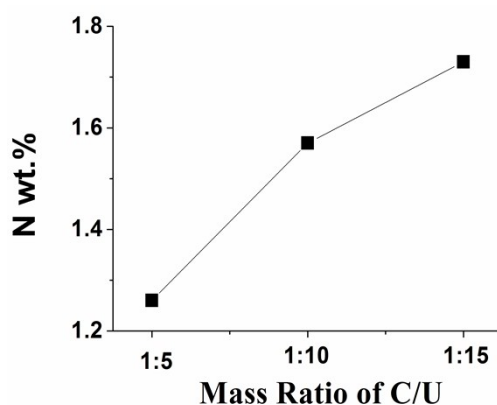


Figure S3. The dependence of final N content on initial C/U ratio.

This figure shows, at the optimal C/U ratio of 1:10, the final N content is about 1.57 wt.% .

3. Typical LSV curves and Tafel plots.

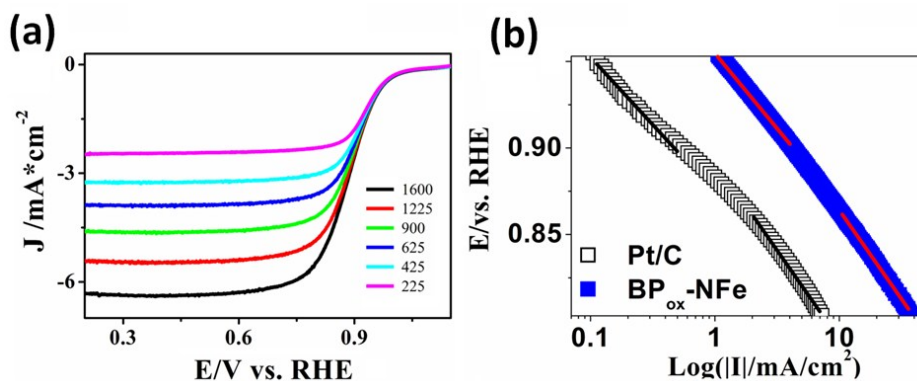


Figure S4. (a) LSV for oxygen reduction on BP_{ox} -NFe in O_2 -saturated 0.1 M KOH at various rotation speeds with scan rate of 5 mV/s. (b) Diffusion-corrected Tafel plots for BP_{ox} -NFe and Pt/C extracted from (b) in Fig.2; the current “I” equals $i_L i / (i - i_L)$, i_L is the limiting current. The loadings of catalysts are 0.39 mg cm^{-2} for doped carbon catalysts and 24 $\mu g_{Pt} cm^{-2}$ for commercial Pt/C.

4. The comparison of alkaline direct methanol fuel cells with different cathode catalysts.

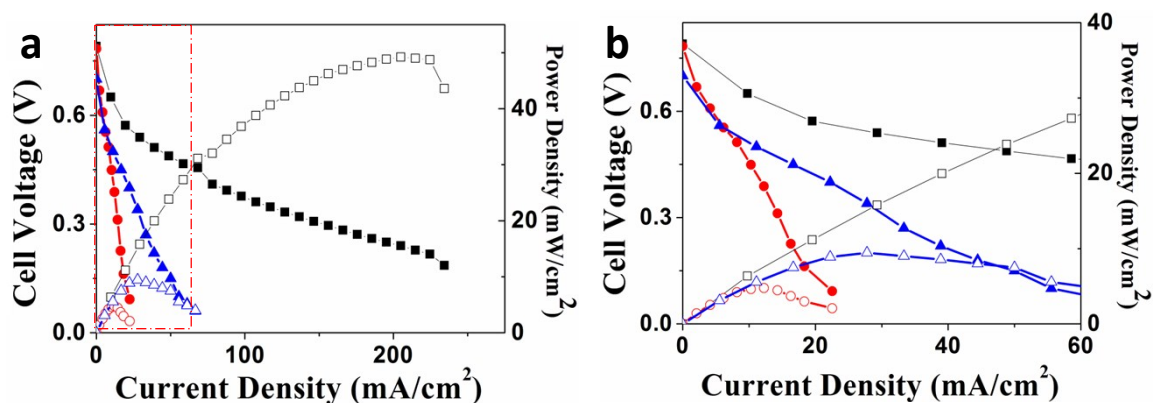


Figure S5. (a) Comparison of ADMFC performance among different cathode catalysts. Red dots (○●) (*J. Appl. Electrochem.*, **2006**, *36*, 25): the performance of a ADMFC with Pt loading 2 mg cm⁻² for both anode and cathode on Na⁺-conducting Nafion 117 membrane. Cell tested at 60°C with 2M methanol and 1M NaOH. Air pressure: 2 bar. Blue triangles (△▲): The voltage and power density of ADMFCs at 60°C with commercial Pt/C (60 wt %, 3 mg_{Pt}/cm²) as anode and cathode with 2 M methanol in 2 M KOH and a flow rate of 5 mL/min, cathode: dry oxygen with flow rate of 100 mL/min. Black squares (□■): The voltage and power density of ADMFCs at 60°C with optimal BP_{ox}-NFe (3 mg/cm²) as cathode. Anode: Pt/C (60 wt %, 3 mg_{Pt}/cm²) with 2 M methanol in 2 M KOH and a flow rate of 5 mL/min, cathode: dry oxygen with flow rate of 100 mL/min. (b) The magnification of the part indicated by a red square in (a).

As shown above Figure S5, the performance (○●) of a ADMFC with Pt/C (2 mg_{Pt}/cm² at 60°C) as both anode and cathode from Prof. K. Scott (University of Newcastle upon Tyne, *J. Appl. Electrochem.*, **2006**, *36*, 25) shows a $P_{\max} \approx 4.5$ mW/cm² with Na⁺-conducting Nafion 117 membrane. When we increased the Pt loading to 3 mg_{Pt}/cm² at 60°C, the P_{\max} increased to about 10 mW/cm² with self-cross linked alkaline solid polymer electrolyte membrane (xQAPS). With the same condition except that the optimal BP_{ox}-NFe (3 mg/cm²) was used as cathode, a larger $P_{\max} \approx 49$ mW/cm² was obtained here. All these data show that our Pt-free BP_{ox}-NFe is a promising alternative to Pt in alkaline fuel cells for ORR.

5. The performance of optimal BP_{ox}-NFe in 0.5 M H₂SO₄.

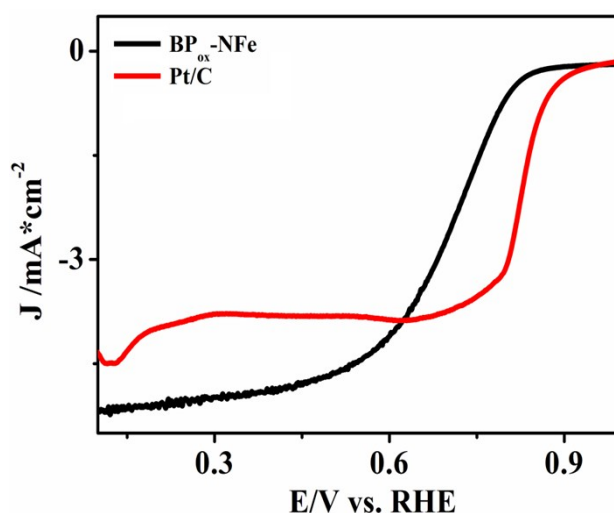


Figure S6. The performance of optimal BP_{ox}-NFe in acid. As a comparison, the performance of commercial Pt/C in acid is also presented. LSV in O₂-saturated 0.5 M H₂SO₄ with rotation speed of 1600 rpm with scan rate of 5 mV/s.

The above optimal BP_{ox}-NFe also show highest electrocatalytic performance in acidic condition for ORR process with onset potential of about 0.89 V vs. RHE. Its performance is on the same level as that obtained based on carbon nanotube-graphene complexes (*Nat. Nanotechnol.* **2012**, *7*, 394). In the present very few reported non-Pt electrocatalysts showed high performance for ORR in both alkaline and acidic conditions.

6. **From the following table we can see that the optimal BP_{ox}-NFe is one of the best catalysts for ORR to date. In this table all the potential values from references were converted to vs.SCE for comparison.**

Table S1. A benchmark of our optimal BP_{ox}-NFe with values obtained from some other independent literatures. All in alkaline condition.

Source/References	Technique	Loading (mg/cm ²)	Activity (SCE)
In this work (<i>N-Fe-co-doped carbon black</i>)	CV, LSV	0.39	E_p = -0.110 V E_{onset} = 0.078 V E_{1/2} = -0.100 V
<i>Nat. Nanotechnol.</i> , 2012, 7, 394-400 (<i>N-Fe-co-doped carbon nanotubes</i>)	LSV	0.485	E_{onset} ≈ 0.060 V
<i>Adv. Mater.</i> 2013, 25, 6879-6883 (<i>N-Fe-co-doped carbon black</i>)	CV, LSV	0.39	E_p = -0.19 V E_{onset} = 0.045 V E_{1/2} = -0.089 V
<i>Nat. Commun.</i> 2013, 4, 1922 (<i>N-Fe-co-doped carbon black</i>)	LSV	1.0	E_{1/2} = -0.089 V

<i>Adv. Mater.</i> 2013, 23, 3192-3196 (N-doped graphene)	LSV	unknown	$E_{\text{onset}} = -0.21 \text{ V}$
<i>Science</i> 2009, 323, 760-764 (N-doped carbon nanotubes)	CV, LSV	unknown	$E_p = -0.22 \text{ V}$ $E_{\text{onset}} \approx 0.00 \text{ V}$
<i>J. Am. Chem. Soc.</i> , 2013, 135, 7823-7826. (N/O-doped mesoporous carbon from PANI/SBA-15)	LSV	0.100	$E_{\text{onset}} = -0.043 \text{ V}$
<i>Angew. Chem. Int. Ed.</i> 2011, 50, 11756-11760 (N-B-co-doped carbon nanotubes)	CV, LSV	unknown	$E_p = -0.3 \text{ V}$ $E_{\text{onset}} = -0.1 \text{ V}$
<i>Sci. Rep.</i> 2013, 3, 2505 (N-F-co-doped carbon black)	CV, LSV	0.39	$E_p = -0.20 \text{ V}$ $E_{\text{onset}} = 0.04 \text{ V}$ $E_{1/2} = -0.12 \text{ V}$
<i>Angew. Chem. Int. Ed.</i> 2011, 50, 3257 – 3261 (P-doped graphite)	CV, LSV	0.1019	$E_p = -0.34 \text{ V}$ $E_{\text{onset}} = 0.043 \text{ V}$
<i>J. Phys. Chem. C</i> , 2013, 117, 24283-24291 (N-doped carbon nanotubes)	LSV	0.21	$E_{\text{onset}} = 0.020 \text{ V}$
<i>Nat. Commun.</i> 2013, 4, 2076 (N-Fe-co-doped carbon nanotubes)	LSV	0.318	$E_{\text{onset}} \approx 0.017 \text{ V}$ $E_{1/2} = -0.068 \text{ V}$
<i>ACS Catal.</i> 2013, 3, 1726–1729 (F-doped carbon black)	CV, LSV	0.39	$E_p = -0.19 \text{ V}$ $E_{\text{onset}} = 0.03 \text{ V}$ $E_{1/2} = -0.158 \text{ V}$
<i>Angew. Chem. Int. Ed.</i> 2012, 51, 4209-4212 (B-N-co-doped graphene)	CV, LSV	Unknown	$E_p = -0.25 \text{ V}$ $E_{\text{onset}} > 0.0 \text{ V}$
<i>Nanoscale</i> , 2013, 5, 3283-3288 (S-N-co-doped carbon)	CV, LSV	Unknown	$E_p = -0.21 \text{ V}$ $E_{\text{onset}} \approx 0.0 \text{ V}$
<i>J. Phys. Chem. C</i> , 2013, 117, 14992–14998 (N-B-co-doped Si rod arrays)	CV, LSV	unknown	$E_p = -0.24 \text{ V}$ $E_{\text{onset}} = -0.09 \text{ V}$ $E_{1/2} = -0.22 \text{ V}$
<i>Langmuir</i> 2013, 29, 13146–13151 (CuCo ₂ O ₄ /N-doped rGO)	CV, LSV	0.30	$E_p = -0.20 \text{ V}$ $E_{\text{onset}} = -0.14 \text{ V}$
<i>Nat. Mater.</i> , 2011, 10, 780-786 (Co ₃ O ₄ /N-doped graphene)	LSV	0.1	$E_{\text{onset}} \approx -0.03 \text{ V}$ $E_{1/2} = -0.153 \text{ V}$
<i>Angew. Chem. Int. Ed.</i> 2011, 50, 5339 – 5343 (CN/Graphene)	CV, LSV	0.0707	$E_p = -0.29 \text{ V}$ $E_{\text{onset}} \approx -0.29 \text{ V}$
<i>Nano Res.</i> 2013, 6(4): 293–301 (N-doped carbon)	CV, LSV	0.10	$E_p = -0.193 \text{ V}$ $E_{\text{onset}} = -0.103 \text{ V}$ $E_{1/2} = -0.193 \text{ V}$

7. A H₂-O₂ fuel cell was tested under a galvanic mode using fully humidified H₂ and O₂ gases flowing with a rate of 250 mL/min and working temperature of 50°C. The related humidity for both H₂ and O₂ was 100%, and the backpressure was 0 MPa. The open circuit voltage (OCV) is up to 0.83 V. The peak power density at this station is up to 107 mW/cm². The maximum power density obtained here is slightly lower than the recently reported best ones for other Fe- or Co-based catalysts (Table S2), but in those cases the performance data were obtained at much higher gas flow rates, higher catalyst loading, higher temperature of 80°C, and even significantly higher backpressure of H₂/O₂ (up to 10 atm) (details see the following Table S2).

In all, it shows that the performance of the optimal catalyst obtained here is among the best ones reported ever.

Table S2. A comparison of our optimal BP_{ox}-NFe with other independent literatures for the performance of alkaline H₂-O₂ fuel cell.

Source/References	Catalysts formation	T (°C)	P _{O2} (atm)	Loading (mg/cm ²)	OCV (V)	Max. Powder density (W/cm ²)
In this work	Fe-based carbon black	50	0	2.0	0.83	0.11
Nature, 2006 , 443, 63	Co-polypyrrole composite	80	2.0	2.0	0.90	0.15
Science, 2011 , 332, 443	Iron/Co-polyaniline derivatives	80	2.71	4.0	0.90	0.55
Sci. Rep., 2013 , 3, 1765	Fe, N-doped carbon with graphene	80	2.04	4.0	0.96	0.33
Angew. Chem. Int. Ed. 2013 , 52, 11755	Pyridinic- and Pyrrolic- Nitrogen-Doped Graphene	80	1.96	4.0	--	0.32
Angew. Chem. Int. Ed. 2014 , 53, 4102	Carbon Nanotubes/ Heteroatom-Doped Carbon Core– Sheath Nanostructures	50	10	2.0	--	0.22

- 8. The performances for the BP_{ox}-Nfe catalysts after various treatment methods have been described below:**

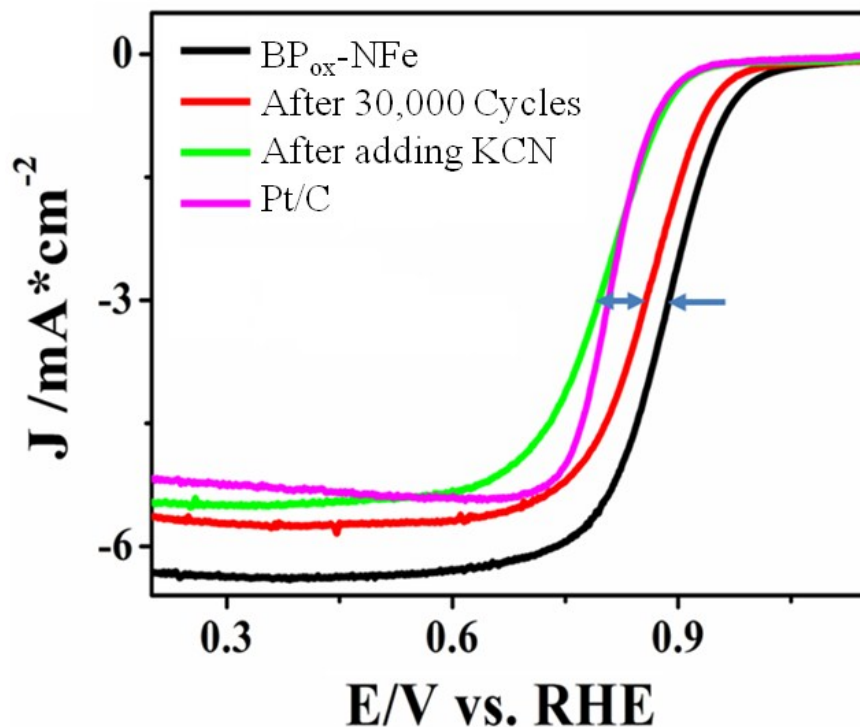


Figure S7. RDE polarization curves of BP_{ox}-NFe with scan rate of 5 mV/s before (black) and after 30,000 potential cycles (red) in O₂-saturated 0.1 M KOH, then KCN was added (green). For comparison, RDE of Pt/C in O₂-saturated 0.1 M KOH was also added (magenta).

9. Raman spectrum of BP_{ox} and BP_{ox}-NFe

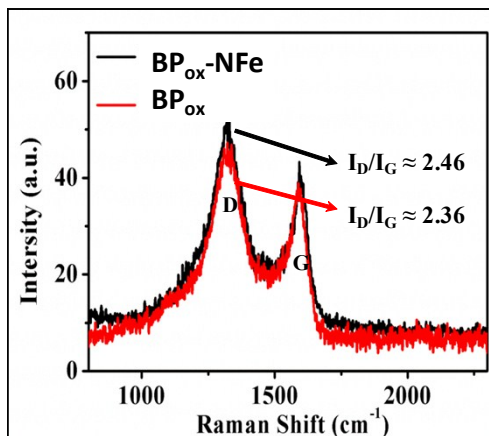


Figure S8. Raman spectrum of BP_{ox} and BP_{ox}-NFe

The Raman Spectra (Figure S8) show the co-doping of N, Fe did not change much the morphology of carbon support.

10. XRD analysis of optimal BPox-NFe.

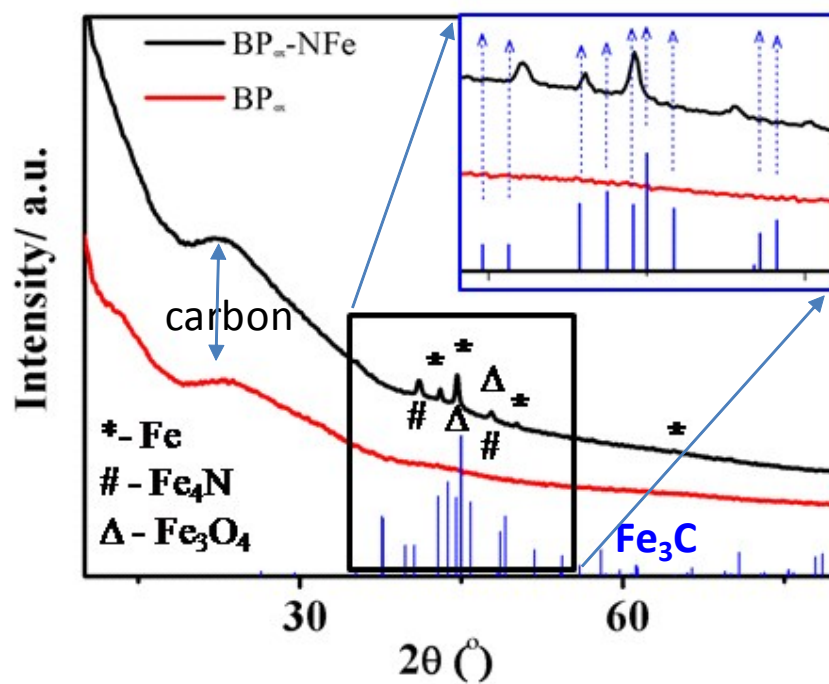


Figure S9. The XRD spectra for BP_{ox} and $\text{BP}_{\text{ox}}\text{-NFe}$ catalysts. The blue column is the peak locations for standard Fe_3C (iron carbide). The inset is the magnification and shows there is no Fe_3C in $\text{BP}_{\text{ox}}\text{-NFe}$.

S1. M. J. Fisch et al., Revision C.01; Gaussian, Inc., Wallingford, CT, **2010**.

S2. R. A. Sidik, A. B. Anderson, N. P. Subramanian, S. P. Kumaraguru, B. N. Popov. *J. Phys. Chem. B* **2006**, *110*, 1787-1793.